Bayesian model selection on scalar ϵ-field dark energy

J. Alberto Vázquez,[1,*] David Tamayo,[2,3,†] Anjan A. Sen,[4,‡] and Israel Quiros[5,§]

[1]*Instituto de Ciencias Físicas, Universidad Nacional Autónoma de México, Cuernavaca, Morelos 62210, Mexico*

[2]*Facultad de Ciencias en Física y Matemáticas, Universidad Autónoma de Chiapas, Tuxtla Gutiérrez, Chiapas 29050, Mexico*

[3]*Mesoamerican Centre for Theoretical Physics, Universidad Autónoma de Chiapas, Tuxtla Gutierrez, Chiapas 29050, Mexico*

[4]*Centre for Theoretical Physics, Jamia Millia Islamia, New Delhi 110025, India*

[5]*Departamento Ingeniería Civil, División de Ingeniería, Universidad de Guanajuato, Guanajuato, C.P. 36000, México*

(Received 7 September 2020; accepted 12 January 2021; published 3 February 2021)

The main aim of this paper is to analyze minimally coupled scalar fields—quintessence and phantom—as the main candidates to explain the accelerated expansion of the Universe and compare its observables to current cosmological observations; as a byproduct we present its PYTHON module. This work includes a parameter ϵ which allows to incorporate both quintessence and phantom fields within the same analysis. Examples of the potentials, so far included, are $V(\phi) = V_0\phi^\mu e^{\beta\phi^\alpha}$ and $V(\phi) = V_0(\cosh(\alpha\phi) + \beta)$ with α, μ, and β being free parameters, but the analysis can be easily extended to any other scalar field potential. Additional to the field component and the standard content of matter, the study also incorporates the contribution from spatial curvature (Ω_k), as it has been the focus in recent studies. The analysis contains the most up-to-date data sets along with a nested sampler to produce posterior distributions along with the Bayesian evidence, that allows to perform a model selection. In this work, we constrain the parameter space describing the two generic potentials, and among several combinations, we found that the best fit to current data sets is given by a model slightly favoring the quintessence field with potential $V(\phi) = V_0\phi^\mu e^{\beta\phi}$ with $\beta = 0.22 \pm 1.56$, $\mu = -0.41 \pm 1.90$, and slightly negative curvature $\Omega_{k,0} = -0.0016 \pm 0.0018$, which presents deviations of 1.6σ from the standard lambda cold dark matter (ΛCDM) model. Even though this potential contains three extra parameters, the Bayesian evidence $\mathcal{B}_{\Lambda,\phi} = 2.0$ is unable to distinguish this model compared to the ΛCDM with curvature ($\Omega_{k,0} = 0.0013 \pm 0.0018$). The potential that provides the minimal Bayesian evidence corresponds to $V(\phi) = V_0\cosh(\alpha\phi)$ with $\alpha = -0.61 \pm 1.36$.

DOI: 10.1103/PhysRevD.103.043506

I. INTRODUCTION

In the standard cosmological model, dark energy (DE) is considered as the source that drives the current accelerated expansion of the Universe and also the dominant component, being around 70% of the total matter-energy content. The observational evidence and theoretical consistency of DE are well supported; for a review, see [1]. However, being either a material fluid or geometry, the physical mechanism behind DE is still a mystery. The simplest model for the DE is the cosmological constant added to the Einstein field equations. This idea with the addition of the cold dark matter (CDM) component are the foundations of the standard cosmological model or ΛCDM. Despite being the simplest approach and even if the ΛCDM model fits well the current cosmological observations, it has been shown that a cosmological constant carries several issues of fundamental nature collectively known as "cosmological constant problems" [2–8]. This points out that the cosmological constant as DE needs a deeper study from fundamental physics and perhaps it is an approximation from a more complex model.

An alternative to the cosmological constant are the so-called dynamical DE models, where the DE equation of state (EOS) has the form of a barotropic perfect fluid $p = w(t)\rho$. In ΛCDM, the EOS parameter w of DE is a constant, $w_\Lambda = -1$, and hence implies a constant energy density, $\rho_\Lambda = \text{const.}$ with a constant negative pressure $p_\Lambda = -\rho_\Lambda$; in contrast, dynamical DE with varying $w(t)$ gives an evolving energy density, i.e., $\rho(t)$. Furthermore, model-independent techniques, based on observational data and on the minimal assumptions, are able to reconstruct

*javazquez@icf.unam.mx
†tamayo.ramirez.d.a@gmail.com
‡aasen@jmi.ac.in
§iquiros@fisica.ugto.mx

the DE EOS and the results are in favor of a dynamical (time-dependent) EOS [9–13]. The dynamical DE models provide alternatives to alleviate the cosmological constant problem among other important current conundrums in cosmology, like the recent H_0 tension [14,15].

Within this approach, scalar fields play a very important role and lead to particular dynamical DE models such as quintessence [16–24], phantom DE [25–30], k-essence [31–34], quintom DE [35–39], among many others. The main idea consists of introducing a scalar field whose associated energy density is able to mimic the cosmological constant at late times. The most popular scalar field DE models contain a single minimally coupled scalar field with a kinetic energy term, where the positive sign corresponds to quintessence and the negative for phantom, and a given scalar field potential. The energy density is the sum of the kinetic energy and the potential whereas their difference results in the effective pressure. The potential of the scalar field supplies the required negative pressure to drive the accelerated expansion of the Universe and its evolution; consequently, the time evolution of the EOS depends crucially on the functional form of the potential.

In this work, we focus on two scenarios: quintessence and phantom. Quintessence is a canonical scalar field minimally coupled to gravity [16]; it is considered as the simplest scenario with no theoretical problems such as the appearance of ghosts or Laplacian instabilities, it describes a time-evolving DE which alleviates the cosmological constant problem. For instance, the so-called "coincidence problem," namely, why the dark matter and dark energy density happen to be of the same order today [40]. Phantom, on the other hand, is a noncanonical scalar field in which the kinetic energy is negative [41–45], despite the "wrong" sign of the kinetic term, phantom models are able to resolve the H_0 tension [41]; meanwhile, in [44], the viability of phantom fields is demonstrated, even when quantum effects are taken into account. This is a very important result since one of the strongest criticisms to the phantom fields is the fact that, since their kinetic energy density is negative, at first sight, one cannot construct a healthy quantum theory of this field. But, in [44], up to first order perturbations in a FLRW background, the authors computed the expectation value of the field's kinetic energy, demonstrating that there is a region in the parameter space where it is not a negative quantity.

As mentioned before, the functional form of the potential $V(\phi)$ determines the time evolution of the scalar field and, consequently, also that of $w(z)$. Since we do not have yet a derivation of $V(\phi)$ from cosmological principles, the common approach is to propose functional forms of the potential inspired from particle physics, mostly in a phenomenological manner, to see how it fits to the data and solves some cosmological challenges. In the literature, there is a plethora of proposals for scalar field potential for late time acceleration [5,24,46–52]. Given a potential, one can always constrain its parameters using the current available set of cosmological data. A step further is to test a collection of potentials and compare its statistical viability in terms of current observations [53–58].

Following this aim, instead of studying a particular scalar field DE potential or a group of them, in this work we propose two generic forms of potentials: $V(\phi) = V_0\phi^\mu e^{\beta\phi^\alpha}$ and $V(\phi) = V_0(\cosh(\alpha\phi) + \beta)$ (α, μ, and β being free parameters). The advantage of our proposal is that it encompasses several potentials proposed in the literature; for specific combinations of values of the free parameters, these generic potentials reproduce known scalar field potentials, for both quintessence and phantom cases depending on a switch parameter ϵ, which will be shown in the following section. In addition, we also use the spatial curvature density parameter $\Omega_{k,0}$ as a free parameter.

The paper is organized as follows. In Sec. II, we set up the mathematical background of minimally coupled scalar fields in cosmology and its description as a dynamical system, we then introduce the switch parameter ϵ in order to have a joint description of quintessence and phantom. In Sec. III, we estimate the initial conditions of the variables of the dynamical system to be solved. We present the generic potentials and their links with other particular potentials in Sec. IV, and in Sec. V, we introduce the code used throughout the analysis and the observational data sets included. In Sec. VI, we show the posteriors of the Bayesian analysis, the constraints of the model parameters in several particular cases, and a model comparison through the Bayesian evidence. Finally, in Sec. VII, a summary of our results and an outlook for future research is given.

Along this work, we use the units $\hbar = c = 8\pi G = 1$.

II. SCALAR FIELD EQUATIONS

The action of a cosmological model including a minimally coupled single scalar field ϕ, either quintessence or phantom, is

$$S = \int d^4x\sqrt{-g}\left[\frac{R}{2} + \epsilon\frac{1}{2}\partial^\nu\phi\partial_\nu\phi - V(\phi) + \mathcal{L}_M\right],$$

where g is the determinant of the metric $g_{\mu\nu}$, R is the Ricci scalar, and the term $\mathcal{L}_M$ accounts for the other matter components of the Universe (namely dark matter, baryons, radiation, etc.). Here, to distinguish the type of field, we have introduced the switch parameter

$$\epsilon = \begin{cases} +1 & \text{quintessence,} \\ -1 & \text{phantom.} \end{cases} \tag{1}$$

Considering a FLRW Universe, the Friedmann equations are thus

$$H^2 + \frac{k}{a^2} = \frac{1}{3}(\rho_\phi + \rho_M), \tag{2}$$

$$\dot{H} - \frac{k}{a^2} = -\frac{1}{2}(\rho_\phi + p_\phi + \rho_M + p_M), \tag{3}$$

where $H = \dot{a}/a$, a is the scale factor, over-dot describes time derivative $\dot{x} = dx/dt$, and k the intrinsic curvature. The standard matter components, $\rho_M = \sum \rho_i$, are assumed as perfect fluids and have a barotropic EOS of the form $p_i = w_i \rho_i$; hence, the usual energy conservation equation for each one reads as

$$\dot{\rho}_i + 3H(1 + w_i)\rho_i = 0. \tag{4}$$

In the case of pressureless matter, we have $w_i = 0$, whereas for the relativistic particles $w_i = 1/3$; similarly, the curvature can be considered as an effective perfect fluid with equation of state $w_i = -1/3$, and move it to the right-hand-side on the expressions (2) and (3). For the scalar field, the effective energy density and pressure are given by

$$\rho_\phi = \epsilon \frac{1}{2}\dot{\phi}^2 + V(\phi), \tag{5}$$

$$p_\phi = \epsilon \frac{1}{2}\dot{\phi}^2 - V(\phi). \tag{6}$$

The associated EOS of the scalar field then becomes

$$w_\phi = \frac{\epsilon\dot{\phi}^2 - 2V(\phi)}{\epsilon\dot{\phi}^2 + 2V(\phi)}, \tag{7}$$

whose value can be determined from the evolution of the field itself that satisfies the Klein-Gordon equation

$$\ddot{\phi} + 3H\dot{\phi} + \epsilon V_{,\phi} = 0, \tag{8}$$

where $x_{,\phi} = dx/d\phi$. Following previous papers [50,59–62], the equations of motion are written in the form of a dynamical system by introducing the variables

$$\Omega_i = \frac{\rho_i}{3H^2}, \qquad \Omega_\phi = \frac{\rho_\phi}{3H^2},$$
$$\lambda = -\epsilon \frac{V_{,\phi}}{V}, \qquad \Gamma = V\frac{V_{,\phi\phi}}{V_{,\phi}^2}. \tag{9}$$

The minus sign in the definition of λ corresponds to $\dot{\phi} > 0$ ($V_{,\phi} < 0$) (for the opposite there would be a plus sign) such that λ remains positive; for further details, see [63]. This convention allows to write ϵ in terms of the potential and its derivative through the *sign* function

$$\epsilon = \text{sign}(-\partial_\phi \ln V(\phi)), \tag{10}$$

and we can then introduce

$$\tilde{\epsilon} \equiv -\partial_\phi \ln V(\phi) = \begin{cases} > 0 & \text{quintessence}, \\ < 0 & \text{phantom}, \end{cases} \tag{11}$$

such that

$$\lambda = \tilde{\epsilon}\epsilon = \tilde{\epsilon}\,\text{sign}(\tilde{\epsilon}). \tag{12}$$

Thus, both types of fields are identified in a single function $\tilde{\epsilon}$. Important to stress out, there is no crossing of the phantom divide line, but this parameter allows to put both models within the same analysis. This approach will also be useful when combining both types of fields, i.e., quintom models.

Therefore, the dynamical system to solve turns out to be

$$\Omega_i' = -3\Omega_i\left(1 + w_i + \frac{2}{3}\frac{\dot{H}}{H^2}\right),$$
$$\Omega_\phi' = -3\Omega_\phi\left(1 + w_\phi + \frac{2}{3}\frac{\dot{H}}{H^2}\right),$$
$$w_\phi' = -(1 - w_\phi)\left(3(1 + w_\phi) - \tilde{\epsilon}\sqrt{3\Omega_\phi(1 + w_\phi)\text{sign}(\tilde{\epsilon})}\right),$$
$$\tilde{\epsilon}' = -\tilde{\epsilon}^2(\Gamma - 1)\sqrt{3\Omega_\phi(1 + w_\phi)\text{sign}(\tilde{\epsilon})}, \tag{13}$$

where prime indicates derivative with respect to the e-fold number $x' \equiv dx/d\ln a$. The last term of the first two equations of (13) is written as

$$-\frac{\dot{H}}{H^2} = q + 1 = \frac{3}{2}\left[\sum_i w_i\Omega_i + w_\phi\Omega_\phi + 1\right], \tag{14}$$

where q is the deceleration parameter, and we have made used of the Friedmann equation

$$1 = \sum_i \Omega_i + \Omega_\phi. \tag{15}$$

The associated equation of state of the scalar field can be described as a deviation of the cosmological constant,

$$w_\phi = -1 + \text{sign}(\tilde{\epsilon})\gamma, \tag{16}$$

with a positive function γ. Moreover, the value of $\tilde{\epsilon}$ will identify the type of field to be considered, either quintessence (+1) or phantom (−1), and hence the terms within the square root $[(1 + w_\phi)\text{sign}(\tilde{\epsilon})]$ in the dynamical system will remain positive.

Notice that not all equations in the dynamical system (13) are linearly independent, i.e., either one of the components of the matter fluids Ω_i, or the scalar field component Ω_ϕ, can be written as a linear combination of the remaining ones. Hence, the dimension of the phase

space equals $d = 3 + (N-1) = N + 2$, where N is the number of matter fields. As in our case, since we choose only two additional components (matter and curvature), then, the derivative of the curvature term, corresponding to $\Omega_k = \rho_k/(3H^2)$, is given by the first expression in (13)

$$\Omega_k' = -3\Omega_k\left(1 - \frac{1}{3} + \frac{2}{3}\frac{\dot{H}}{H^2}\right). \tag{17}$$

Also, in (14), both the matter and curvature contribution will be given by $\sum_i w_i\Omega_i = -\Omega_k/3$, and due to the Friedmann constraint (15), we can eliminate Ω_m in the dynamical system. Therefore, the independent phase-space variables are, Ω_ϕ, w_ϕ, $\tilde{\epsilon}$, and Ω_k, i.e., the phase space is four-dimensional (4D). The dimension of the phase space can be further reduced if an exponential potential is chosen since, in these cases, $\tilde{\epsilon}$ is a constant, as we shall see in the next section.

III. INITIAL CONDITIONS

Even though the system can be extended for any amount of components-i, for the sake of this work we restrict to a Universe made of a scalar field, dust (dark matter + baryons), and curvature, and considering a smooth transition to the radiation domination epoch (photons and three neutrino species, $N_{\rm eff} = 3.046$, with minimum allowed mass $\sum m_\nu = 0.06$ eV).

Some papers pointed out the sensitivity of the initial conditions in order to get accurate results [29]. There have been several approaches for the conditions, for instance, by assuming a general potential $V(\phi) = V_0 f(\phi)$, in [53] used V_0, ϕ_0, $\dot{\phi}_0$ as free parameters for the initial conditions, additional to the parameters that describe the form of the potential.

In our case, the initial conditions can be set up right into the matter domination epoch ($a_{\rm ini} \sim 10^{-3}$) and we are considering the initial conditions that realize thawing behavior (the field is initially frozen at the flat part of the potential due to large Hubble friction and behaves like cosmological constant $w = -1$ [60]), then we are able to choose the initial EOS of the scalar field ($w_{\phi,\rm ini}$) very close to the cosmological constant. Therefore, from Eq. (16), we keep fixed $\gamma_{\rm ini} = 10^{-4}$, for either sign of $\tilde{\epsilon}$.

The initial value for the field density parameter, $\Omega_{\phi,\rm ini}$, can be taken as a free parameter. However, we tested this process and adding an extra parameter will reduce the acceptance rate in the analysis and therefore increase the computation time considerably. Thus, to enhance the process and minimize the computation time, $\Omega_{\phi,\rm ini}$ is thus selected such that its present value is $\Omega_{\phi,0} = 1 - \sum_i \Omega_{i,0}$. This can easily be achieved with a shooting method.

The parameter $\tilde{\epsilon}_{\rm ini}$ will decide the type of field in place and can be either chosen as a sampling parameter or instead of taking the initial value of the field $\phi_{\rm ini}$. We performed a Bayesian analysis by using both parameters and the results, as expected, will produce similar constraints on the base parameters. However, the selection of using $\phi_{\rm ini}^{-1}$ provides a slightly better fit and less correlated constraints over the selection of $\tilde{\epsilon}_{\rm ini}$.

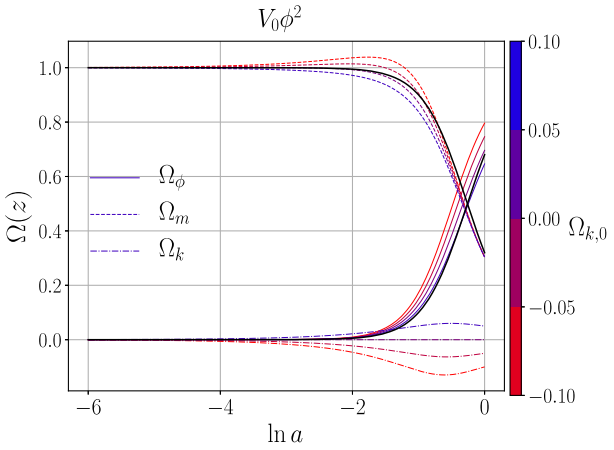

FIG. 1. Density parameters for a Universe where DE is described by a quintessence field with potential $V(\phi) = V_0\phi^2$, dust described by dark matter + dust (Ω_m), and a curvature component (Ω_k) color coded to span the range of $\Omega_{k,0} = [-0.1, 0.1]$. Black solid lines describe the flat-ΛCDM model by using the current Planck values.

To illustrate the whole process, Fig. 1 displays the density parameters for a Universe where DE is described by a quintessence field ($\tilde{\epsilon}_{\rm ini} > 0$) with potential $V(\phi) = V_0\phi^2$, dust describes the dark matter + baryons (Ω_m), and a curvature component (Ω_k) is color coded to span the range $\Omega_{k,0} = [-0.1, 0.1]$. The initial conditions are fixed right into the matter domination epoch. Black solid lines describe the flat-ΛCDM model by using the current Planck values.

IV. POTENTIALS

The main aim of this work is to study a general potential, for either quintessence or phantom, and compare its observables with current cosmological observations, and then to include a PYTHON module into the SimpleMC code [64,65]. As a proof of the concept, here we focus on two general classes of potentials that comprise a wide variety of fundamental models of particular importance for cosmology. First, let us explore the three-parametric class of potentials: (a) $V(\phi) = V_0\phi^\mu e^{\beta\phi^\alpha}$ and then the two-parametric class: (b) $V(\phi) = V_0(\cosh(\alpha\phi) + \beta)$.

The generic potential (a) under particular choices of the parameters μ, β, and α boils down into potentials already studied in the literature. Here, α, λ, χ, γ being positive constant values, we have

A. $V(\phi) = V_0\phi^\mu e^{\beta\phi^\alpha}$.

For quintessence,

(i) $\mu = -\alpha$, $\beta = 0$: $V(\phi) = V_0 M_{pl}^2 \phi^{-\alpha}$ [46].
(ii) $\mu = 0$, $\beta = -\lambda/M_{pl}$, $\alpha = 1$: $V(\phi) = V_0 \exp[-\lambda\phi/M_{pl}]$ [47].
(iii) $\mu = -\chi$, $\beta = \gamma/M_{pl}^2$, $\alpha = 2$: $V(\phi) = V_0\phi^{-\chi}\exp[\gamma\phi^2/M_{pl}^2]$ [48].
(iv) $\mu = 0$, $\beta = M_{pl}$, $\alpha = -1$: $V(\phi) = V_0\exp[M_{pl}/\phi]$ [24].

For phantom,

(i) $\mu = 6$, $\beta = 0$: $V(\phi) = V_0\phi^6$ [50].
(ii) $\mu = -2$, $\beta = 0$: $V(\phi) = V_0\phi^{-2}$ [50].
(iii) $\mu = 0$, $\alpha = 1$: $V(\phi) = V_0 e^{\beta\phi}$ [50].
(iv) $\mu = 2$ $\beta = 0$: $V(\phi) = V_0\phi^2$ [51].

In [53], the authors make a joint study about several of these potentials.

Similarly, for the second potential,

B. $V(\phi) = V_0(\cosh(\alpha\phi) + \beta)$.

(i) $\beta = 1$, $\alpha = i/f$: $V(\phi) = V_0(\cos(\phi/f) + 1)$ [52].
(ii) $\beta = -1$: $V(\phi) = V_0(\cosh(\alpha\phi) - 1)$ [66].
(iii) $\beta = 0$: $V(\phi) = V_0\cosh(\alpha\phi)$ [67].

In general, several of these potentials have been also studied in the context of dark matter and inflation, for instance, $V_0\phi^2$ [61], $V_0\lambda\phi^4$ [68], $V_0(\cosh(\lambda\phi) - 1)$ [69], $V_0(a\cos(\phi/f) + 1)$ [70], $V_0 e^{\phi^2}(\phi - \phi_0)^2$ [71].

Notice that once we specify the scalar field potential, we are able to compute $\tilde{\epsilon}$ and Γ [given in the expression (9)] and hence the dynamical system (13) will be closed. For the potential $V(\phi) = V_0\phi^\mu e^{\beta\phi^\alpha}$, we have the $\tilde{\epsilon}$ and Γ functions are, respectively,

$$-\tilde{\epsilon} = \mu\phi^{-1} + \alpha\beta\phi^{\alpha-1},$$
$$\Gamma = 1 + \frac{1}{\tilde{\epsilon}^2}[\alpha(\alpha-1)\beta\phi^{\alpha-2} - \mu\phi^{-2}], \tag{18}$$

and similarly for $V(\phi) = V_0(\cosh(\alpha\phi) + \beta)$, we have

$$-\tilde{\epsilon} = \frac{\alpha\sinh(\alpha\phi)}{\cosh(\alpha\phi) + \beta},$$
$$\Gamma = -\frac{\alpha}{\tilde{\epsilon}}\coth(\alpha\phi). \tag{19}$$

With these quantities in mind, the free parameters can be sampled over and find out their constraints. To cover several of the aforementioned parameters, and furthermore, Table I shows some of these particular cases. Figure 2 displays, for the potentials we focus on, the general behavior of its equation of state along with the $H(z)/(1+z)$ function. Green error bars correspond to the galaxy and Ly-α BAO, as we shall explain below.

TABLE I. Selected parameters and the model they described, along with the auxiliary variables $\tilde{\epsilon}$ and Γ.

β	μ	α	Model	$\tilde{\epsilon}$	Γ
β	0	1	$e^{\beta\phi}$	$-\beta$	1
0	μ	–	ϕ^μ	$-\mu\phi^{-1}$	$1-\frac{1}{\mu}$
β	0	2	$e^{\beta\phi^2}$	$-2\beta\phi$	$1+\frac{2\beta}{\tilde{\epsilon}^2}$
β	μ	1	$\phi^\mu e^{\beta\phi}$	$-(\mu\phi^{-1}+\beta)$	$1-\frac{1}{\mu}(1+\frac{\beta}{\tilde{\epsilon}})^2$
β	0	α	$e^{\beta\phi^\alpha}$	$-\alpha\beta\phi^{\alpha-1}$	$1+\frac{(\alpha-1)}{\alpha\beta}(-\frac{\tilde{\epsilon}}{\alpha\beta})^{\frac{\alpha}{1-\alpha}}$
β	2	2	$\phi^2 e^{\beta\phi^2}$	$-2(\phi^{-1}+\beta\phi)$	$\frac{3}{4}+\frac{4\beta}{\tilde{\epsilon}^2}\mp\frac{\sqrt{\tilde{\epsilon}^2-16\beta}}{4\tilde{\epsilon}}$
0	$\cdots$	α	$\cosh(\alpha\phi)$	$-\alpha\tanh(\alpha\phi)$	$\frac{\tilde{\epsilon}^2}{\alpha^2}$
-1	$\cdots$	α	$\cosh(\alpha\phi)-1$	$-\alpha\coth(\frac{\alpha\phi}{2})$	$\frac{1}{2}(1+\frac{\alpha^2}{\tilde{\epsilon}^2})$
1	$\cdots$	$i\alpha$	$\cos(\alpha\phi)+1$	$\alpha\tan(\frac{\alpha\phi}{2})$	$\frac{1}{2}(1-\frac{\alpha^2}{\tilde{\epsilon}^2})$

V. CODE AND DATA SETS

To explore the parameter space and impose constraints on the free parameters, we use the new version of the SimpleMC code [64,65]. The code already contains several samplers for a proper exploration of the parameter space, but in particular we use a modified version of the nested sampler Dynesty [72–74] that allows to explore complex posterior distributions and to compute the Bayesian evidence, which is used to perform a model comparison through the Jeffreys scale [75]. The Bayesian evidence has been used in several papers to compare DE models, parametrizations for the DE EOS, inflationary models, and to perform reconstructions of cosmological functions, among many other applications; see, for instance, [9,10,75,76]. For a comprehensive review of the parameter inference in cosmology, see Ref. [77]. Throughout this analysis, we use the recent baryon acoustic oscillations (BAO) data sets from Ly-α DR14, BAO-galaxy consensus, MGS, and 6dFGS as presented in [78–83], a collection of currently available cosmic chronometers that provides measurements of the Hubble function (see [84] and references therein), a compressed version of the Pantheon data set which speeds up the process without losing accuracy [85], and a compressed version of Planck-15 information (treated as a BAO experiment located at redshift $z = 1090$, [65]) to improve constraints and break degeneracies.

The flat priors of the base parameters used throughout the analysis correspond to $\Omega_{m,0} = [0.05, 0.5]$ for the matter density parameter today, $\Omega_{b,0}h^2 = [0.02, 0.025]$ for the physical baryon density parameter, $h = [0.4, 1.0]$ for the reduced Hubble constant, and $\Omega_{k,0} = [-0.03, 0.03]$ for the effective curvature density parameter today. Whereas to select the priors that described the potential parameters we based upon Fig. 2 which displays general behaviors for the functions $w(z)$ and $H(z)/(1+z)$ by varying some of

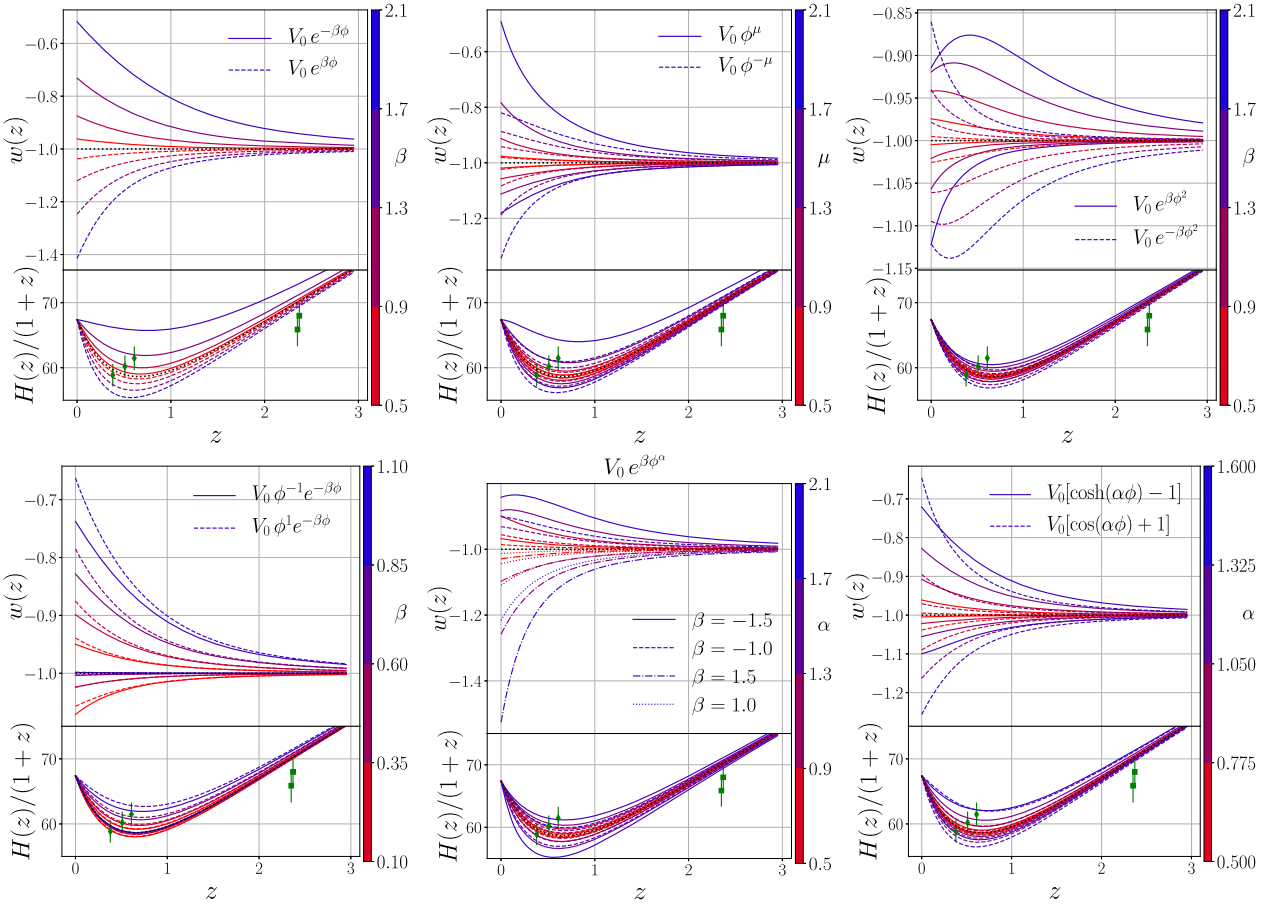

FIG. 2. Evolution of the DE EOS parameter $w(z)$ for selected values of the parameters of the generic potentials (both quintessence and phantom) and $H(z)/(1+z)$, along with data from BAO galaxy consensus and Ly-α DR14.

these parameters. Hence, the flat priors we selected for the potential parameters are $\mu = [-6, 6]$, $\beta = [-3, 3]$, $\alpha = [-3, 3]$, $\phi_{\rm ini}^{-1} = [-3, 3]$.

VI. RESULTS

Figure 4 shows the 2D marginalized posterior distributions with scatter points color coded accordingly with the parameter on the right colored bar. Notice that each panel contains two colors that represent the type of field: phantom (blue) and quintessence (red), depending on the sign of $\tilde{\epsilon}_{\rm ini}$ and therefore on the combination of parameters for each potential. In almost all the presented models, except for the $\cos(\alpha\phi) + 1$ model, we notice the center of the 2D posterior distribution is slightly inclined to the quintessence field.

Within the potentials studied, the mean value of the Hubble parameter is around $H_0 = 68$ km/s/Mpc which is consistent with the value of the ΛCDM model. Despite the diversity of potentials and even if the phantom regime is considered, there is not a significant departure from the standard background cosmology that may allow to alleviate the H_0 tension. If we see Fig. 3, up to 2σ, $w(z = 0)$ can go at most till -1.1 which is insufficient to shift the central

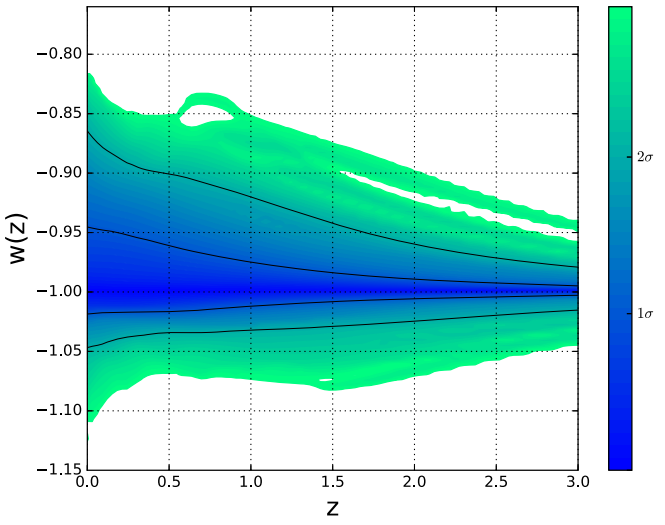

FIG. 3. This panel shows the posterior probability $Pr(w|z)$ for the potential that best fits to the data ($V = V_0 \phi^{\mu} e^{\beta\phi}$): the probability of w as normalized in each slice of constant z, with color scale in confidence interval values. Solid lines describe 1σ (68%) and 2σ (95%) confidence contour levels.

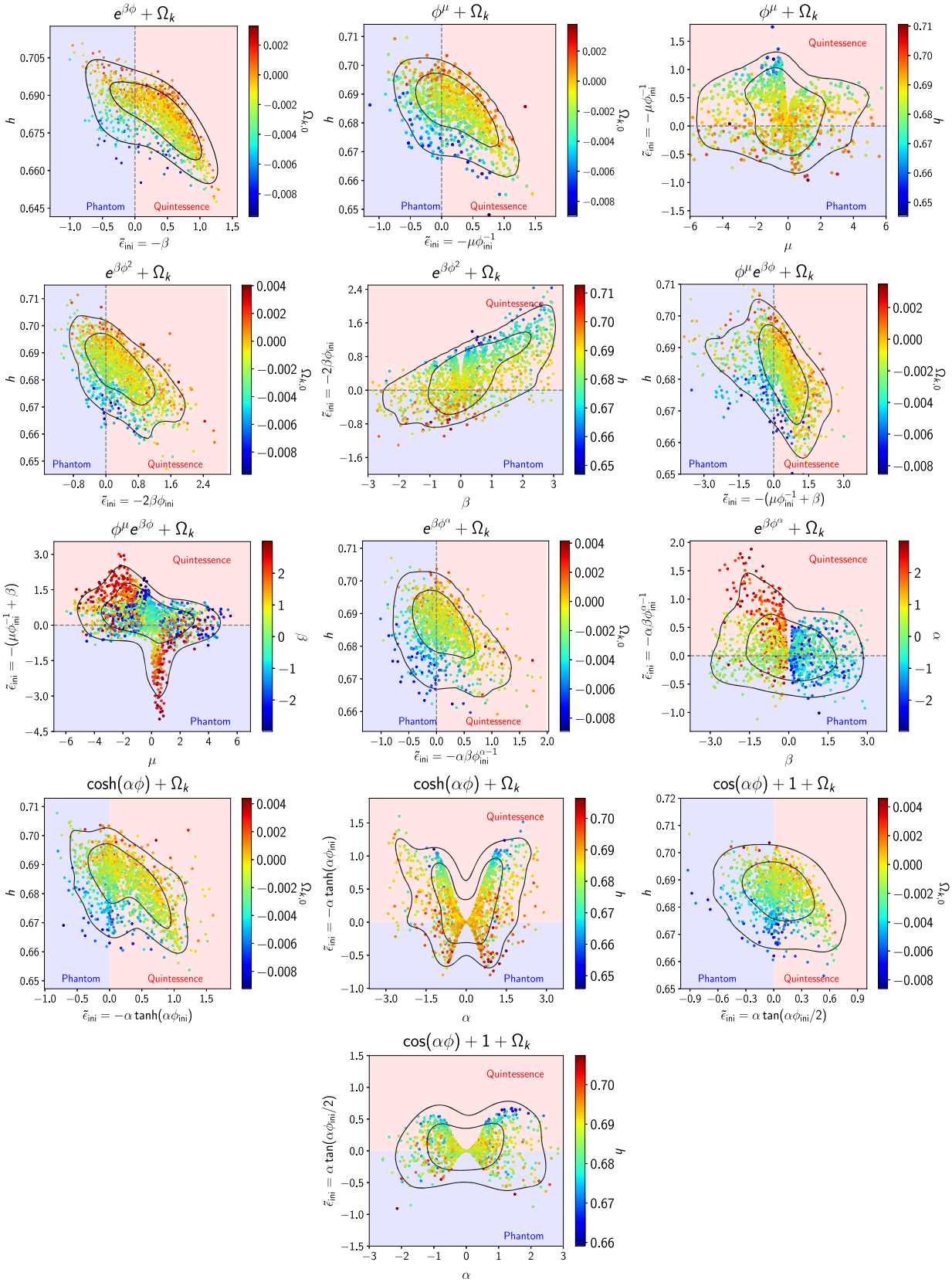

FIG. 4. 2D marginalized posterior distributions for each set of parameters given and potential. Color blue represents models laying on the phantom region, whereas red those models in the quintessence. Inner (outer) contours describe 1σ (68%) and 2σ (95%) confidence contour levels.

TABLE II. Mean values along with 1σ constraints on the set of parameters used to described each model. For one-tailed distributions, the upper limit 95% C.L. is given. For two tailed, the 68% C.L. is shown. Before the last column, $-2\ln\mathcal{L}_{,\max}$ is used to compare best fit with respect to the ΛCDM model. The last column contains the Bayesian evidence.

Model	$\Omega_{m,0}$	h	$\Omega_{k,0}$	$\phi_{\rm ini}^{-1}$	β	μ	α	$\tilde{\epsilon}_{\rm ini}$	$-2\ln\mathcal{L}_{\max}$	$\ln\mathcal{Z}$
ΛCDM	0.3005(68)	0.6830(53)	0	⋯	⋯	⋯	⋯	⋯	60.44	−40.39(20)
ΛCDM + k	0.3008(67)	0.6849(65)	0.0013(18)	⋯	⋯	⋯	⋯	⋯	59.30	−41.10(22)
$e^{\beta\phi}$	0.3023(91)	0.6838(98)	0	⋯	−0.37(43)	0	1	0.37(43)	59.00	−40.81(21)
$e^{\beta\phi}+k$	0.3026(86)	0.6812(95)	−0.0016(17)	⋯	−0.34(44)	0	1	0.34(44)	58.46	−42.02(23)
ϕ^{μ}	0.3009(79)	0.6856(85)	0	0.15(91)	0	−0.13(2.13)	⋯	0.29(42)	58.94	−40.95(22)
$\phi^{\mu}+k$	0.3001(78)	0.6842(83)	−0.0016(18)	0.31(96)	0	−0.31(1.88)	⋯	0.22(41)	58.32	−42.05(23)
$e^{\beta\phi^2}$	0.3003(78)	0.6863(83)	0	−0.13(96)	0.39(1.07)	0	2	0.36(55)	58.32	−41.36(22)
$e^{\beta\phi^2}+k$	0.3011(80)	0.6832(87)	−0.0015(17)	−0.17(99)	0.34(1.11)	0	2	0.34(56)	58.18	−42.18(23)
$\phi^{\mu}e^{\beta\phi}$	0.3013(82)	0.6850(90)	0	0.23(1.29)	0.25(1.52)	−0.37(2.17)	1	0.32(90)	58.44	−41.41(22)
$\phi^{\mu}e^{\beta\phi}+k$	0.3019(82)	0.6820(90)	−0.0016(18)	0.27(1.31)	0.22(1.56)	−0.41(1.90)	1	0.26(92)	58.02	−42.42(23)
$e^{\beta\phi^{\alpha}}$	0.2989(73)	0.6879(75)	0	0.18(0.93)	−0.04(1.27)	0	0.11(1.28)	0.19(42)	58.48	−41.67(22)
$e^{\beta\phi^{\alpha}}+k$	0.2993(71)	0.6853(74)	−0.0017(18)	0.15(1.01)	−0.05(1.15)	0	0.09(1.22)	0.12(39)	58.22	−42.57(23)
$\cosh(\alpha\phi)$	0.30087(80)	0.6858(85)	0	−0.31(1.00)	0	⋯	−0.61(1.36)	0.34(46)	58.50	−40.63(21)
$\cosh(\alpha\phi)+k$	0.30090(79)	0.6835(85)	−0.0016(18)	−0.43(1.31)	0	⋯	0.02(93)	0.26(41)	58.14	−41.47(22)
$\cos(\alpha\phi)+1$	0.2977(66)	0.6895(61)	0	0.23(1.41)	1	⋯	0.01(1.03)	0.06(69)	59.12	−40.76(21)
$\cos(\alpha\phi)+1+k$	0.2992(69)	0.6855(73)	−0.0018(18)	0.07(0.94)	1	⋯	0.38(1.33)	0.14(58)	58.54	−41.48(22)

value of H_0, as has been shown in [86] that it is needed $w(z=0)$ around -1.3 to shift the central value of H_0 toward 70–71.

Finally, an important point to stress out is the presence of pronounced degeneracies over the parameter space. For instance, in the model with potential $V(\phi)=V_0e^{\beta\phi^{\alpha}}$, the parameter space is divided into two regions, one with $\beta>0,\alpha<0$ and the other one with $\beta<0,\alpha>0$ and in the center of this region $V(\phi)=V_0$. Something similar happens with the potential $V(\phi)=V_0\phi^{\mu}e^{\beta\phi}$. A notable feature for this case is the fact that the points do not cluster near the center of the confidence curve, and also clearly the particular case $\beta=0$ is constrained by the initial condition to $\tilde{\epsilon}_{ini}\sim 0$. These types of degeneracies are very complex and time consuming to explore within the standard Markov Chain Monte Carlo methods, hence the use of nested samplers. To complement this figure, Table II contains mean values along with 1σ constraints on the set of parameters used to described each model. Looking at the mean values of $\tilde{\epsilon}$, we obtain that in general there is a slight inclination to quintessence models ($\tilde{\epsilon}>0$) for an open Universe ($\Omega_{k,0}<0$) (also observed in Fig. 4).

In terms of particular models, the potential $V=V_0e^{\beta\phi}$ slightly favors β negative (positive for quintessence and negative for phantom values); in contrast, the potential $V=V_0e^{\beta\phi^2}$ slightly favors β, which means there is a maximum in the equation of state. For $V=V_0e^{\beta\phi^{\alpha}}$, the parameters $\beta\approx 0.16$ and $\alpha\approx 0.1$, all either for flat or curved Universe; notice that the power $\alpha\approx 0.1$ of the last case lies between the powers 0 and 2 of the first and second cases. For the power-law potential, $V=V_0\phi^{\mu}$, models with an exponent $|\mu|>2$ lay down right on the 1σ limits. The model with a potential $V=V_0\phi^{\mu}e^{\beta\phi}$, the means are located at $\beta\sim 0.2$ and $\mu\sim -0.4$, this potential with negative curvature provides a better fit to the data compared to the rest of the models and shows and improvement of 1.6σ with respect to the ΛCDM model, however with three extra parameters. The potential $V=V_0\cosh(\alpha\phi)$ has the feature that the best fit of the parameter α is negative in the flat case and positive in a Universe with curvature case with a slightly preference to an open Universe. Finally, for the potential $V=V_0(\cos(\alpha\phi)+1)$, the parameters $\alpha\sim 0$ and $\alpha\sim 0.4$ for the flat and curvature cases, respectively.

Last column contains the Bayesian evidence ($\ln\mathcal{Z}$), and according to Jeffrey's scale, the models are indistinguishable and hence still consistent with ΛCDM. In general, we found that scalar field models preferred an open Universe compared to positive curvature for the ΛCDM model.

VII. CONCLUSIONS

In this paper, we have been able to incorporate minimally coupled scalar fields—quintessence and phantom—into the same analysis with the use of a switch parameter $\tilde{\epsilon}$ and then to present it as a PYTHON module for the SimpleMC code [64]. The variables introduced here allow us to write down the dynamical system in terms of variables that naturally simplify the selection of initial conditions. This $\tilde{\epsilon}$ parameter will be useful when the two fields are combined, i.e., quintom models. For the proof of the concept, we have considered two generic classes of potentials, a three-parametric class $V(\phi)=V_0\phi^{\mu}e^{\beta\phi^{\alpha}}$ and also the two-parametric class $V(\phi)=V_0(\cosh(\alpha\phi)+\beta)$, but the code can easily be extended to more specific

potentials. One of the objectives of the code is to enable the study of very general models of scalar dark energy potentials such as the one presented in this work. We found that for the combined data set, the preferred model corresponds to $V = V_0\phi^\mu e^{\beta\phi}$ and negative curvature. For this potential, Fig. 3 contains the posterior probability of the equation of state $Pr(w|z)$: the probability of w as normalized in each slice of constant z, with color scale in confidence interval values [87]. The Bayesian evidence points out an inconclusive difference among models. For the coming data sets, this work may be able to identify the type of field and the scalar field potential that best describes observations.

ACKNOWLEDGMENTS

J. A. V. acknowledges the support provided by FOSEC SEP-CONACYT Investigación Básica A1-S-21925, FORDECYT-PRONACES/304001/2020, and UNAM-DGAPA-PAPIIT IA102219. D. T. acknowledges the receipt of the grant from the Abdus Salam International Centre for Theoretical Physics, Trieste, Italy and would like to thank Karen Caballero for the hospitality provided at the Facultad de Ciencias en Física y Matemáticas, Universidad Autónoma de Chiapas. A. A. S. acknowledges funding from DST-SERB, Govt of India, under the Project No. MTR/2019/000599.

[1] D. Huterer and D. L. Shafer, Rep. Prog. Phys. **81**, 016901 (2018).
[2] P. J. E. Peebles and B. Ratra, Astrophys. J. Lett. **325**, L17 (1988).
[3] S. Weinberg, Rev. Mod. Phys. **61**, 1 (1989).
[4] A. G. Riess *et al.* (Supernova Search Team), Astron. J. **116**, 1009 (1998).
[5] I. Zlatev, L. M. Wang, and P. J. Steinhardt, Phys. Rev. Lett. **82**, 896 (1999).
[6] S. M. Carroll, Living Rev. Relativity **4**, 1 (2001).
[7] P. J. E. Peebles and B. Ratra, Rev. Mod. Phys. **75**, 559 (2003).
[8] T. Padmanabhan, Phys. Rep. **380**, 235 (2003).
[9] J. Alberto Vazquez, M. Bridges, M. P. Hobson, and A. N. Lasenby, J. Cosmol. Astropart. Phys. 09 (2012) 020.
[10] S. Hee, J. A. Vázquez, W. J. Handley, M. P. Hobson, and A. N. Lasenby, Mon. Not. R. Astron. Soc. **466**, 369 (2017).
[11] G. B. Zhao *et al.*, Nat. Astron. **1**, 627 (2017).
[12] Y. Wang, L. Pogosian, G. B. Zhao, and A. Zucca, Astrophys. J. **869**, L8 (2018).
[13] David Tamayo and J. Alberto Vazquez, Mon. Not. R. Astron. Soc. **487**, 729 (2019).
[14] W. Yang, S. Pan, E. Di Valentino, E. N. Saridakis, and S. Chakraborty, Phys. Rev. D **99**, 043543 (2019).
[15] S. Pan, W. Yang, E. Di Valentino, E. N. Saridakis, and S. Chakraborty, Phys. Rev. D **100**, 103520 (2019).
[16] S. Tsujikawa, Classical Quantum Gravity **30**, 214003 (2013).
[17] S. M. Carroll, Phys. Rev. Lett. **81**, 3067 (1998).
[18] L. M. Wang and P. J. Steinhardt, Astrophys. J. **508**, 483 (1998).
[19] L. Amendola, Phys. Rev. D **62**, 043511 (2000).
[20] T. Chiba, T. Okabe, and M. Yamaguchi, Phys. Rev. D **62**, 023511 (2000).
[21] L. M. Wang, R. R. Caldwell, J. P. Ostriker, and P. J. Steinhardt, Astrophys. J. **530**, 17 (2000).
[22] W. Zimdahl and D. Pavon, Phys. Lett. B **521**, 133 (2001).
[23] L. P. Chimento, A. S. Jakubi, D. Pavon, and W. Zimdahl, Phys. Rev. D **67**, 083513 (2003).
[24] R. Caldwell and E. V. Linder, Phys. Rev. Lett. **95**, 141301 (2005).
[25] R. R. Caldwell, Phys. Lett. B **545**, 23 (2002).
[26] R. R. Caldwell, M. Kamionkowski, and N. N. Weinberg, Phys. Rev. Lett. **91**, 071301 (2003).
[27] E. Elizalde, S. Nojiri, and S. D. Odintsov, Phys. Rev. D **70**, 043539 (2004).
[28] S. Nojiri, S. D. Odintsov, and S. Tsujikawa, Phys. Rev. D **71**, 063004 (2005).
[29] J. Kujat, R. J. Scherrer, and A. A. Sen, Phys. Rev. D **74**, 083501 (2006).
[30] K. J. Ludwick, Mod. Phys. Lett. A **32**, 1730025 (2017).
[31] T. Chiba, Phys. Rev. D **66**, 063514 (2002).
[32] M. Malquarti, E. J. Copeland, A. R. Liddle, and M. Trodden, Phys. Rev. D **67**, 123503 (2003).
[33] R. J. Scherrer, Phys. Rev. Lett. **93**, 011301 (2004).
[34] L. P. Chimento and A. Feinstein, Mod. Phys. Lett. A **19**, 761 (2004).
[35] Z. K. Guo, Y. S. Piao, X. M. Zhang, and Y. Z. Zhang, Phys. Lett. B **608**, 177 (2005).
[36] H. Wei, R. G. Cai, and D. F. Zeng, Classical Quantum Gravity **22**, 3189 (2005).
[37] B. Feng, M. Li, Y. S. Piao, and X. M. Zhang, Phys. Lett. B **634**, 101 (2006).
[38] W. Zhao, Phys. Rev. D **73**, 123509 (2006).
[39] Y. F. Cai, E. N. Saridakis, M. R. Setare, and J. Q. Xia, Phys. Rep. **493**, 1 (2010).
[40] L. P. Chimento, A. S. Jakubi, D. Pavon, and W. Zimdahl, Phys. Rev. D **67**, 083513 (2003); R. G. Cai and A. Wang, J. Cosmol. Astropart. Phys. 03 (2005) 002; B. Hu and Y. Ling, Phys. Rev. D **73**, 123510 (2006); S. Dodelson, M. Kaplinghat, and E. Stewart, Phys. Rev. Lett. **85**, 5276 (2000).
[41] G. Alestas, L. Kazantzidis, and L. Perivolaropoulos, arXiv:2004.08363.
[42] A. Bouali, I. Albarran, M. Bouhmadi-López, and T. Ouali, Phys. Dark Universe **26**, 100391 (2019).
[43] D. Perkovic and H. Stefancic, Phys. Lett. B **797**, 134806 (2019).
[44] K. J. Ludwick, Phys. Rev. D **98**, 043519 (2018).

[45] N. Roy and N. Bhadra, J. Cosmol. Astropart. Phys. 06 (2018) 002.
[46] B. Ratra and P. Peebles, Phys. Rev. D **37**, 3406 (1988).
[47] P. G. Ferreira and M. Joyce, Phys. Rev. D **58**, 023503 (1998).
[48] P. Brax and J. Martin, Phys. Lett. B **468**, 40 (1999).
[49] H. Y. Chang and R. J. Scherrer, arXiv:1608.03291.
[50] R. J. Scherrer and A. Sen, Phys. Rev. D **78**, 067303 (2008).
[51] S. Dutta and R. J. Scherrer, Phys. Lett. B **676**, 12 (2009).
[52] S. Dutta and R. J. Scherrer, Phys. Rev. D **78**, 123525 (2008).
[53] O. Avsajanishvili, Y. Huang, L. Samushia, and T. Kahniashvili, Eur. Phys. J. C **78**, 773 (2018).
[54] J. B. Durrive, J. Ooba, K. Ichiki, and N. Sugiyama, Phys. Rev. D **97**, 043503 (2018).
[55] A. I. Lonappan, S. Kumar, Ruchika, B. R. Dinda, and A. A. Sen, Phys. Rev. D **97**, 043524 (2018).
[56] N. Roy, A. X. Gonzalez-Morales, and L. A. Urena-Lopez, Phys. Rev. D **98**, 063530 (2018).
[57] F. Tosone, B. S. Haridasu, V. V. Lukovi, and N. Vittorio, Phys. Rev. D **99**, 043503 (2019).
[58] W. Yang, M. Shahalam, B. Pal, S. Pan, and A. Wang, Phys. Rev. D **100**, 023522 (2019).
[59] R. Lazkoz, G. Leon, and I. Quiros, Phys. Lett. B **649**, 103 (2007).
[60] R. J. Scherrer and A. A. Sen, Phys. Rev. D **77**, 083515 (2008).
[61] T. Matos, A. Vazquez-Gonzalez, and J. Magana, Mon. Not. R. Astron. Soc. **393**, 1359 (2009).
[62] T. Gonzalez, T. Matos, I. Quiros, and A. Vazquez-Gonzalez, Phys. Lett. B **676**, 161 (2009).
[63] T. Chiba, Phys. Rev. D **73**, 063501 (2006).
[64] Temporarily stored at: https://github.com/ja-vazquez/SimpleMC.
[65] E. Aubourg *et al.*, Phys. Rev. D **92**, 123516 (2015).
[66] V. Sahni and L.-M. Wang, Phys. Rev. D **62**, 103517 (2000).
[67] L. Arturo Urena-Lopez and T. Matos, Phys. Rev. D **62**, 081302 (2000).
[68] L. E. Padilla, J. Alberto Vázquez, T. Matos, and G. Germán, J. Cosmol. Astropart. Phys. 05 (2019) 056.
[69] T. Matos, J.-R. Luevano, I. Quiros, L. Arturo Urena-Lopez, and J. Alberto Vazquez, Phys. Rev. D **80**, 123521 (2009).
[70] G. G. Ross, G. German, and J. Alberto Vazquez, J. High Energy Phys. 05 (2016) 010.
[71] G. Germán, J. C. Hidalgo, F. X. Linares Cedeo, A. Montiel, and J. Alberto Vázquez, Phys. Rev. D **101**, 023507 (2020).
[72] J. S. Speagle, Mon. Not. R. Astron. Soc. **493**, 3132 (2020).
[73] J. Skilling, AIP Conf. Proc. **735**, 395 (2004).
[74] J. Skilling, Bayesian Anal. **12**, 855 (2006).
[75] J. Alberto Vazquez, A. N. Lasenby, M. Bridges, and M. P. Hobson, Mon. Not. R. Astron. Soc. **422**, 1948 (2012).
[76] J. Alberto Vazquez, M. Bridges, M. P. Hobson, and A. N. Lasenby, J. Cosmol. Astropart. Phys. 06 (2012) 006.
[77] L. E. Padilla, L. O. Tellez, L. A. Escamilla, and J. Alberto Vazquez, arXiv:1903.11127.
[78] S. Alam *et al.* (BOSS Collaboration), Mon. Not. R. Astron. Soc. **470**, 3 (2017).
[79] M. Blomqvist *et al.*, Astron. Astrophys. **629**, A86 (2019).
[80] M. Ata *et al.*, Mon. Not. R. Astron. Soc. **473**, 4773 (2018).
[81] V. de Sainte Agathe *et al.*, Astron. Astrophys. **629**, A85 (2019).
[82] F. Beutler, C. Blake, M. Colless, D. Heath Jones, L. Staveley-Smith, L. Campbell, Q. Parker, W. Saunders, and F. Watson, Mon. Not. R. Astron. Soc. **416**, 3017 (2011).
[83] L. Anderson *et al.*, Mon. Not. R. Astron. Soc. **441**, L1 (2014).
[84] A. Gómez-Valent and L. Amendola, J. Cosmol. Astropart. Phys. 04 (2018) 051.
[85] D. M. Scolnic *et al.*, Astrophys. J. **859**, 101 (2018).
[86] S. Vagnozzi, Phys. Rev. D **102**, 023518 (2020).
[87] W. Handley, J. Open Source Softw. **3**, 849 (2018).